Deficiency of Phosphoinositide 3-Kinase Enhancer Protects Mice From Diet-Induced Obesity and Insulin Resistance

Chi Bun Chan,[1] Xia Liu,[1] Dae Young Jung,[2,3] John Y. Jun,[2] Hongbo R. Luo,[4] Jason K. Kim,[2,3] and Keqiang Ye[1]

OBJECTIVE—Phosphoinositide 3-kinase enhancer A (PIKE-A) is a proto-oncogene that promotes tumor growth and transformation by enhancing Akt activity. However, the physiological functions of PIKE-A in peripheral tissues are unknown. Here, we describe the effect of *PIKE* deletion in mice and explore the role of PIKE-A in obesity development.

RESEARCH DESIGN AND METHODS—Whole-body PIKE knockout mice were generated and subjected to high-fat–diet feeding for 20 weeks. The glucose tolerance, tissue-specific insulin sensitivity, adipocyte differentiation, and lipid oxidation status were determined. The molecular mechanism of PIKE in the insulin signaling pathway was also studied.

RESULTS—We show that PIKE-A regulates obesity development by modulating AMP-activated protein kinase (AMPK) phosphorylation. PIKE-A is important for insulin to suppress AMPK phosphorylation. The expression of PIKE-A is markedly increased in adipose tissue of obese mice, whereas depletion of PIKE-A inhibits adipocyte differentiation. *PIKE* knockout mice exhibit a prominent phenotype of lipoatrophy and are resistant to high-fat diet–induced obesity, liver steatosis, and diabetes. *PIKE* knockout mice also have augmented lipid oxidation, which is accompanied by enhanced AMPK phosphorylation in both muscle and adipose tissue. Moreover, insulin sensitivity is improved in PIKE-A–deficient muscle and fat, thus protecting the animals from diet-induced diabetes.

CONCLUSIONS—Our results suggest that PIKE-A is implicated in obesity and associated diabetes development by negatively regulating AMPK activity. ***Diabetes*** **59:883–893, 2010**

From the [1]Department of Pathology and Laboratory Medicine, Emory University School of Medicine, Atlanta, Georgia; the [2]Department of Cellular and Molecular Physiology, Pennsylvania State University College of Medicine, Hershey, Pennsylvania; the [3]Program in Molecular Medicine and Department of Medicine, Division of Endocrinology, Metabolism and Diabetes, University of Massachusetts Medical School, Worcester, Massachusetts; and the [4]Department of Pathology and Lab Medicine, Harvard Medical School and Children's Hospital Boston, Boston, Massachusetts.

Corresponding author: Keqiang Ye, kye@emory.edu.

Received 21 September 2009 and accepted 21 December 2009. Published ahead of print at http://diabetes.diabetesjournals.org on 12 January 2010. DOI: 10.2337/db09-1404.

Obesity is a result of imbalanced energy intake and expenditure in which the accumulation of excessive fat causes disorders such as type 2 diabetes, atherosclerosis, and dyslipidemia (1). Because of its increasing prevalence in most of the world, obesity has became a major health problem (2). Although genetic linkage analysis has successfully mapped potential loci in human genome for adiposity development (3), identifying all genetic variants that contribute to differences in body weight is still one of the major goals to fully understand the mechanism of obesity progression. Recent studies using genome-wide linkage scan revealed human chromosome trait 12q14.1, where the phosphatidylinositol 3-kinase (PI 3-kinase) enhancer (PIKE) gene *CENTG1* locates, has a strong correlation with serum lipid level and energy intake (4,5), suggesting PIKE may be a potential factor in regulating body weight.

PIKEs are a family of GTPases that directly interact with PI 3-kinase and Akt and enhance their kinase activities (6–8). The family contains three members: PIKE-L, PIKE-S, and PIKE-A, which is generated from alternative splicing of the *CENTG1* gene. Whereas PIKE-S and -L are brain specific, PIKE-A is widely expressed, such that its mRNA could be detected in brain, heart, liver, muscle, spleen, thymus, and small intestine (9,10). The mode of action of PIKE is isoform specific in different cell types. PIKE-L couples to receptors such as netrin receptor (UNC5B) and metabotropic glutamate receptors I (mGluR-I) and links the activated receptor to PI 3-kinase pathway in neurons (11,12). PIKE-S localizes in nucleus and executes the protective effects of nerve growth factor by activating the nuclear PI 3-kinase cascade (8). PIKE-A, on the other hand, substantiates the kinase activity of Akt in glioblastomas and is involved in cancer invasion activity (6,13,14). However, the role of PIKE-A in peripheral tissues remains unknown.

In many cases, insulin resistance is the major associated pathologic condition of obesity. However, the molecular mechanism of this obesity-induced disorder remains ambiguous. It has been proposed that lipotoxicity is one of the candidates to explain the role of excess lipid storage in insulin resistance onset. Accumulation of excess cellular lipid changes the lipid metabolism, enhances oxidative stress, and disrupts endoplasmic reticulum homeostasis (15). Increasing cellular lipid oxidation by pharmacologic interventions in obese subjects thus represents a potential therapeutic regimen to mitigate their diabetic complications. In this regard, AMP-activated protein kinase (AMPK) is one of the targets. AMPK is the master sensor for energy status and is responsible for metabolic homeostasis (16).

Activation of AMPK results in reducing hepatic gluconeogenic gene expression and glucose production, increasing fatty acid oxidation, and enhancing glucose uptake. Therefore, AMPK activators such as AICAR and metformin are effective agents in relieving the obesity-induced insulin resistance in both laboratory and clinical tests (17).

To examine the role of PIKE in obesity, we developed the whole-body *PIKE* knockout ($PIKE^{-/-}$) mice with ablation of all PIKE isoforms. Here we report that PIKE-A is implicated in adipocyte differentiation and obesity development. *PIKE* knockout elicits lipoatrophy and increased insulin sensitivity by enhancing AMPK activity, leading to resistance against high-fat diet (HFD)-induced obesity and diabetes.

RESEARCH DESIGN AND METHODS

Generation of knockout animals and genotyping. Heterozygous $PIKE^{+/-}$ C57BL/6 mice with a targeted deletion of exons 3–6 of *CENTG1* were generated under contract by Ozgene (Bentley DC, Australia). Genotyping was performed by PCR using genomic DNA isolated from the tail tip. PCR was performed using a combination of primers D (5′ACAGGATCAGTGCATCATCTC3′), H (5′CTGCCCAGCTACAGGAGTAG3′), A (5′TCAGTTGACTGGAAGCTCTG3′), and C (5′CCAGAGCCTATCTATGCCTAG3′).

Immunoprecipitation and Western blotting. Tissue extracts were prepared by homogenizing the tissues in buffer as reported (18). Immunoprecipitation was performed as described (18). Antibodies used in the Western blot analysis were obtained from Santa Cruz Biotechnology (insulin receptor, Akt) and Cell Signaling Technology (anti–phosphor-Thr^{308} of Akt, anti–phosphor-Thr^{172} of AMPK, anti–phosphor-Ser^{79} of acetyl-CoA carboxylase [ACC], anti-AMPKα, and anti-ACC).

Southern blot analysis. Southern blot analysis using mouse tail genomic DNA was performed as reported (19).

Analytic procedures. All animal experiments were performed according to the care of experimental animal guidelines from Emory University. Twelve-week-old female mice were fed with chow or HFD (Research Diets) for 20 weeks. Blood glucose level was measured by ACCU-CHEK Advantage Blood Glucose Meter (F. Hoffmann-La Roche, Basel, Switzerland). Serum insulin was measured by ELISA (Crystal Chem). Serum triglyceride level was measured by Serum Triglyceride Determination Kit (Sigma-Aldrich). Serum tumor necrosis factor-α (TNF-α) was measured by ELISA (BD Biosciences). Glucose tolerance test (GTT) was performed on mice after peritoneal injection of D-glucose (2 g/kg body wt).

In vivo insulin stimulation. Animals (16 h fasting) were anesthetized by intraperitoneal administration of sodium pentobarbital (50 mg/kg body wt). Saline or 5 units human insulin (Eli Lilly) was injected through inferior vena cava. After 5 min, liver, hind limb muscles, and inguinal fat were removed and immediately frozen in liquid nitrogen.

PI 3-kinase assay. In vitro PI 3-kinase assay was performed using anti-p110α (Santa Cruz Biotechnology) as described previously (8).

RT-PCR. Total RNA from various tissues was prepared by Trizol Isolation Reagent (Invitrogen). First-strand cDNA from total RNA was synthesized using Superscript III reverse transcriptase (Invitrogen) and Oligo-dT_{17} as primer. Amplification of preadipocyte factor 1 (Pref-1), adipocyte protein 2 (aP2), peroxisome proliferator–activated receptor-γ (PPARγ), and C BPα was performed using primers mPref1-F (5′-GACCCACCCTGTGACCCC-3′), mPref1-R (5′-CAGGCAGCTCGTGCACCCC-3′); maP2-F (5′-CAAAATGTGTGATGCCTTTGTG-3′), maP2-R (5′-CTCTTCCTTTGGCTCATGCC-3′); mPPARg2-F (5′-ATGCTGTTATGGGTGAAACT-3′), mPPARg2-R (5′-CTTGGAGCTTCAGGTCATATTTGTA-3′); and mC BPa-F (5′-ATCCCAGAGGGACTGGAGTT-3′), mC BPa-R (5′-AAGTCTTAGCCGGAGGAAGC-3′). Expression of PIKE-A was determined using primers D and H as described above. Glyceraldehyde-3-phosphate dehydrogenase (GAPDH) was also amplified as internal standard using primers 5′-CGCATCTTCTTGTGCAGTGCC-3′ (forward) and 5′-GGCCTTGACTGTGCCGTTGAATTT-3′ (reverse).

In vitro ^{3}H-2-deoxyglucose uptake. ^{3}H-2-deoxyglucose uptake in soleus muscle and inguinal fat pad was performed in the presence or absence of human insulin (Eli Lilly) as reported (20).

Fatty acid oxidation assay. Fatty acid oxidation was measured by determining the production of ^3H_2O from [9,10-^{3}H]-palmitate as reported (21).

Hyperinsulinemic-euglycemic clamp and metabolic cage studies. Metabolic cage studies and in vivo glucose metabolisms including glucose infusion rate, glucose turnover rate, and glycogen synthesis were determined by hyperinsulinemic-euglycemic clamp as reported (22,23).

Statistical analysis. Results were considered significant when $P < 0.05$. Statistical analysis was performed using either Student t test, one-way ANOVA, or two-way ANOVA followed by Tukey multiple comparison test or Bonferroni post-tests using the computer program GraphPad Prism (GraphPad Software).

Detailed experimental procedures are in the supplementary methods (http://diabetes.diabetesjournals.org/cgi/content/full/db09-1404/DC1).

RESULTS

Generation of *PIKE* knockout mice. As a pioneer study on the physiological role of PIKE in obesity development, we generated whole-body $PIKE^{-/-}$ mice with targeted disruption in the *CENTG1* locus using the LoxP/Cre system. We first created a transgenic line with $PIKE^{flox/+}$ allele by inserting two loxP sites into the introns flanking exons 3 and 6 (Fig. 1*A*). $PIKE^{flox/+}$ mice were then bred with transgenic mice expressing Cre recombinase in all tissues. Deletion of exons 3–6 results in removal of GTPase domain and introduces a frameshift mutation that creates a new stop codon, producing truncated PIKE proteins for all isoforms. Heterozygous mating generated newborn pups at expected Mendelian frequency that appeared indistinguishable from the wild-type littermates, suggesting that PIKE was dispensable for embryonic development. Southern blot analysis showed exons 3–6 of the *CENTG1* gene were effectively excised (Fig. 1*B*), which was further supported by PCR analysis (Fig. 1*C*). Immunoblotting analysis using antibody specific to the COOH-terminal of PIKE-A and RT-PCR confirmed the ablation of PIKE-A expression in various tissues (Fig. 1*D* and *E*). $PIKE^{-/-}$ mice are viable and fertile. However, a significant reduction of white adipose tissues (WATs) was detected in the $PIKE^{-/-}$ mice, whereas no noticeable difference was found in other peripheral tissues (Fig. 1*E*).

***PIKE*$^{-/-}$ mice are resistant to diet-induced obesity.** When fed a chow diet, the body weight of female $PIKE^{-/-}$ mice was slightly, but significantly, lower at 8 weeks old compared with wild-type mice (17.29 ± 0.27 vs. 16.33 ± 0.29 g, $P < 0.05$, $n = 7$, Student t test). The difference was more prominent in mice fed with HFD (55% of calories derived from fat). After HFD feeding for 14 weeks, obesity developed in wild-type but not in $PIKE^{-/-}$ animals (Fig. 2*A*). Daily food intake of $PIKE^{-/-}$ mice fed a chow diet was normal, but the amount of food intake in $PIKE^{-/-}$ mice was substantially less than that in the control fed HFD (Fig. 2*B*). Increased body weight was associated with a drastic gain of inguinal WAT weight in wild-type but not in $PIKE^{-/-}$ mice (312% in wild-type vs. 46.5% in knockout) (Fig. 2*C*). The adipocytes in $PIKE^{-/-}$ mice were also smaller in both feeding conditions (Fig. 2*D* and *E*). Moreover, circulating leptin and TNF-α concentrations were lower in $PIKE^{-/-}$ mice (Fig. 2*F* and *G*). Expression of PIKE-A was greatly enhanced in the WAT and muscle of mice fed with HFD and the genetically obese (*ob/ob*) mice (Fig. 2*H*, *first* and *fifth panels*). In contrast, no noticeable alternation of hepatic PIKE expression was detected among all the tested groups (Fig. 2*H*, *third panel*), suggesting a tissue-specific function of PIKE-A in obesity development.

***PIKE* is essential for adipocyte differentiation.** Under chow diet feeding conditions, expressions of mature adipocyte markers aP2 and the master regulators of adipocyte differentiation, PPARγ and C/EBPα (24,25), were reduced in $PIKE^{-/-}$ WAT (Fig. 3*A*). However, no significant difference was found in preadipocyte marker Pref-1 between wild-type and mutant. Comparable increment of

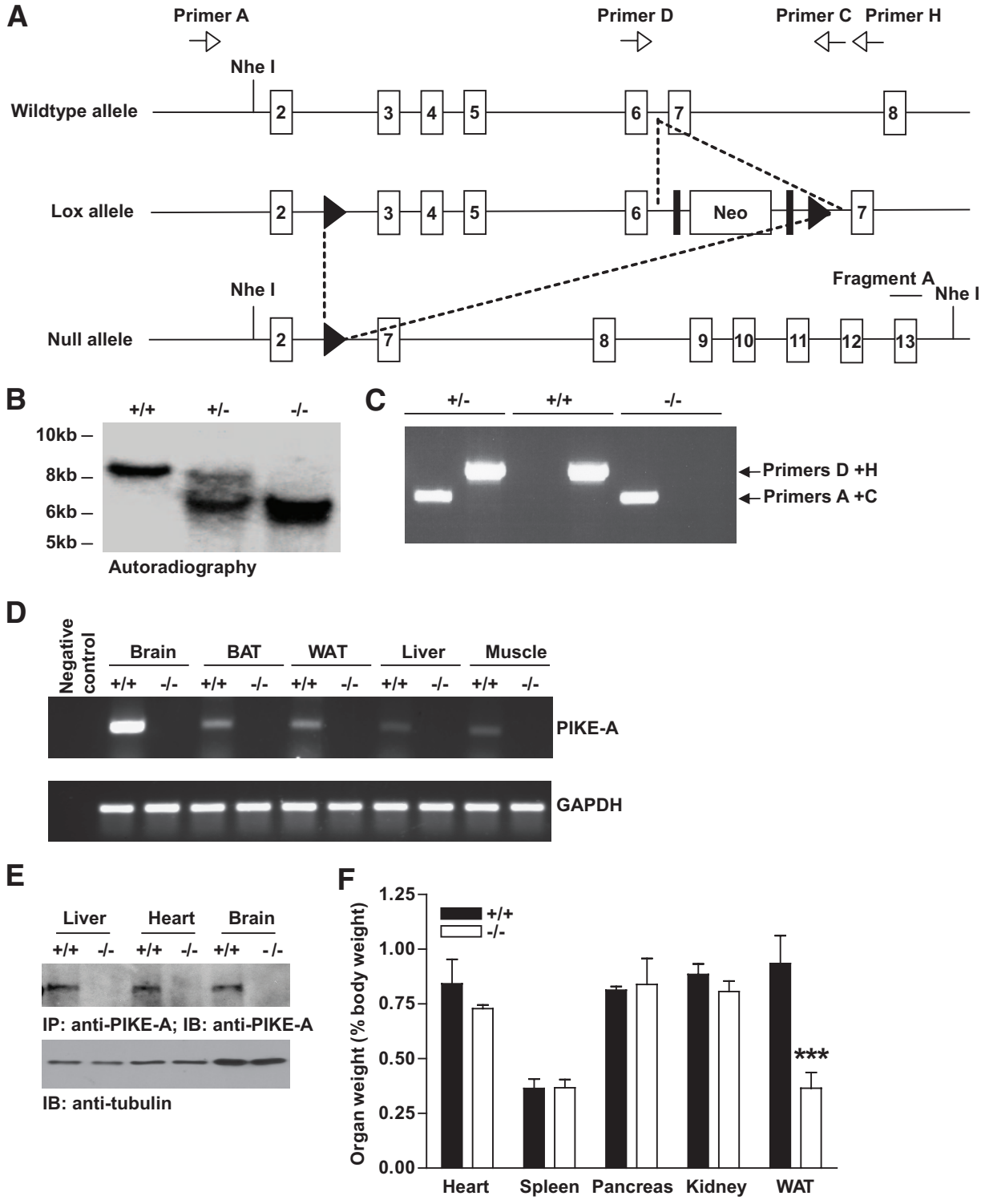

FIG. 1. Targeted disruption of *PIKE*. *A*: Schematic representation of mouse *PIKE* (*top*), the targeting vector (*middle*), and the targeted gene region (*bottom*). The locations of loxP sites were marked as solid triangles and of FRT sites, as solid bars. *B*: Southern blot analysis of progeny produced from heterozygote mating. Genomic DNA was isolated from mouse tail and was digested with *Nhe*I and probed with fragment A as indicated. The 8.5-kb band represents the wild-type allele and the 6-kb fragment corresponds to the knockout allele. *C*: PCR screening of mice from heterozygote mating. Genomic DNA isolated from wild-type (+/+), heterozygous (+/+), and knockout (−/−) mice tail was used in PCR screening. The locations of primers used in the reactions were indicated in *A*. *D*: RT-PCR screening of PIKE expression in different tissues. Complementary DNA was synthesized from RNA extracted from various tissues as indicated. Primers D and H as shown in *A* were used in PCR (*upper panel*). Expression of GAPDH was examined as the internal control (*lower panel*). *E*: Western blot analysis of PIKE-A. Proteins extracts of different tissues from wild-type (+/+) and knockout (−/−) mice (3 months old) were prepared, and the expression of PIKE-A was detected using specific antibody against the COOH-terminal of human PIKE-A (*top panel*). The amount of tubulin in each sample was examined to demonstrate equal loading (*bottom panel*). Representative result of three mice from each genotype was shown. *F*: Weight of heart, spleen, pancreas, kidney, and inguinal WAT in 3-month-old mice. The weight was normalized with the total body weight and was expressed as means ± SEM ($n = 5$). Significant reduction of WAT weight was observed in $PIKE^{-/-}$ mice (*$P < 0.001$, Student t test).**

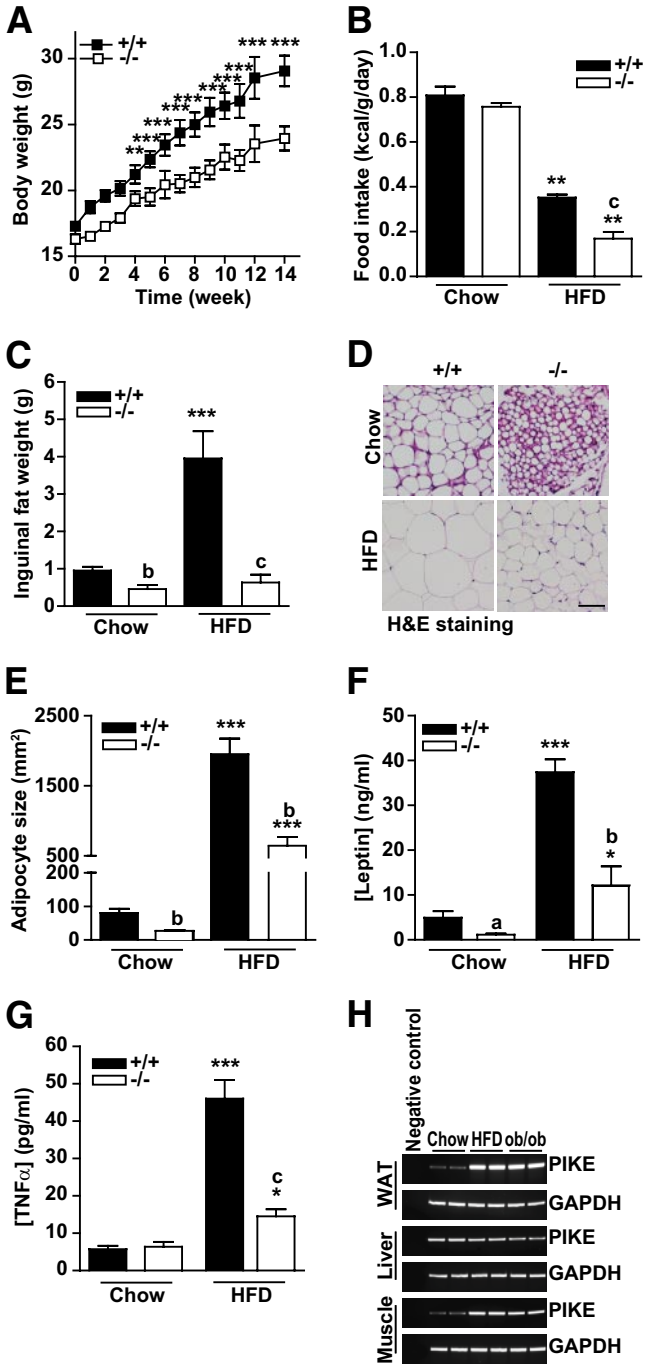

FIG. 2. *PIKE* knockout mice are resistant to diet-induced obesity. *A*: Growth curve of 3-month-old wild-type (+/+) and PIKE knockout (−/−) mice fed with HFD. Body weight was measured weekly and expressed as mean ± SEM (n = 7–10; **P < 0.01, ***P < 0.001, two-way ANOVA). *B*: Food intake by wild-type (+/+) and knockout (−/−) mice fed with chow or HFD was measured in a 3-day period. Results were expressed as mean ± SEM (P < 0.01 vs. the same genotype; c: P < 0.001 vs. the same diet; one-way ANOVA, n = 4). *C*: Weight of inguinal WAT from wild-type (+/+) and *PIKE* knockout (−/−) mice (8–9 months old, n = 5) that have been fed with chow diet or HFD for 20 weeks. Data were expressed as mean ± SEM (***P < 0.001 vs. the same genotype, b: P < 0.01, c: P < 0.001 vs. the same diet treatment; one-way ANOVA). *D*: Pictures of hematoxylin-eosin (H&E) staining of inguinal WAT sections from wild-type (+/+) and PIKE-null (−/−) animals (8–9 months old) that have been fed with chow diet or HFD for 20 weeks. Representative results of three different mice from each genotype were shown. Scale bar represents 50 μm. *E*: Quantification of inguinal WAT cell area from wild-type (+/+) and PIKE-null (−/−) animals (8–9 months old) that have been fed with chow diet or HFD for 20 weeks (n = 4). Results were expressed as mean ± SEM (***P < 0.001 vs. the same genotype, b: P < 0.01 vs. the same diet treatment; one-way ANOVA). *F*: Circulating leptin concentration of wild-type (+/+) and PIKE knockout (−/−) mice (8–9 months old) that have been fed with chow or HFD for 20 weeks. Results were expressed as mean ± SEM (n = 4; *P < 0.05, ***P < 0.001 vs. the same genotype; a: P < 0.05, b: P < 0.01 vs. the same diet treatment; one-way ANOVA). *G*: Circulating TNF-α concentration of wild-type (+/+) and PIKE knockout (−/−) mice (8–9 months old) that have been fed with chow or HFD for 20 weeks. Results were expressed as mean ± SEM (n = 4; *P < 0.05, ***P < 0.001 vs. the same genotype; c: P < 0.01 vs. the same diet treatment; one-way ANOVA). *H*: Elevated PIKE-A expression in the WAT and muscle of diet-induced or genetically obese mice. RNA from WAT, liver, and muscle of *ob/ob* mice or normal mice (8–9 months old) that have been fed with chow diet or HFD was extracted and reverse transcripted. (A high-quality color representation of this figure is available in the online issue.)**

Pref-1 was also detected in both genotypes treated with HFD, suggesting the proliferation of preadipocyte was similar in both genotypes (Fig. 3*A*). However, subsequent adipocyte differentiation was impaired in *PIKE*$^{-/-}$ mice as the expression of aP2, PPARγ, and C/EBPα was greatly reduced.

Next, we sought to determine whether the deletion of PIKE-A per se is sufficient to prevent adipogenesis in vitro. Whereas mouse embryonic fibroblasts (MEFs) from wild-type mice differentiated into adipocytes, as evident by the accumulation of lipid droplets within the cells, *PIKE*$^{-/-}$ MEFs failed to fully differentiate under the same condition (Fig. 3*B*). A significantly lower amount of oil red O staining was found in *PIKE*$^{-/-}$ MEFs after induction (Fig. 3*C*). Moreover, expression of mature adipocyte markers aP2, C/EBPα, and PPARγ was lower in *PIKE*$^{-/-}$ MEFs after differentiation (Fig. 3*D*), which was consistent with the findings in WAT. These results suggest lipoatrophy is a direct consequence of PIKE-A depletion in WAT, which may explain the reduced adiposity of mutant mice.

***PIKE* knockout mice are protected from diet-induced hyperglycemia by enhanced systemic insulin sensitivity.** Adipocyte dysfunction is one of the major factors that causes insulin resistance (26); therefore, we examined the effects of diet-induced diabetes in *PIKE*$^{-/-}$ mice. In HFD treatment, hyperglycemia was observed in both genotypes when the animals were fed. Hyperglycemia was sustained in fasted wild-type animals but not in *PIKE*$^{-/-}$ mice (Fig. 4*A*). Moreover, *PIKE*$^{-/-}$ mice on HFD showed improved glucose tolerance during the GTT (Fig. 4*B*). A lower amount of insulin was also secreted in *PIKE*$^{-/-}$ mice treated with HFD during the GTT (supplementary Fig. 1*A*). In parallel, less circulating insulin was detected in *PIKE*$^{-/-}$ mice in both feeding conditions (Fig. 4*C*), suggesting a higher insulin sensitivity. This notion was further supported by higher glucose infusion rate (Fig. 4*D*), whole-body glucose turnover (supplementary Fig. 1*B*), and glycogen synthesis (supplementary Fig. 1*C*) in *PIKE*$^{-/-}$ mice during the hyperinsulinemic-euglycemic clamp studies. Hepatic insulin resistance was also alleviated in *PIKE*$^{-/-}$ mice fed with HFD (supplementary Fig. 1*D*), which provides further explanation to the relieved diabetic phenotype in *PIKE*$^{-/-}$ mice because hepatic insulin resistance is associated with diabetes (27). We also examined the insulin-stimulated signaling in tissues responsible for glucose utilization to reveal the molecular basis of the enhanced insulin sensitivity in *PIKE*$^{-/-}$ mice. In mice fed a normal chow diet, comparable tyrosine phosphorylation of insulin receptor occurred in WAT and muscle of both genotypes after in vivo insulin injection (Fig. 4*E*, *first panel*). However, insulin provoked higher insulin substrate-1 (IRS-1) phosphorylation, PI 3-kinase activity, and Akt phosphorylation in *PIKE*$^{-/-}$ WAT and muscle (Fig. 4*E*,

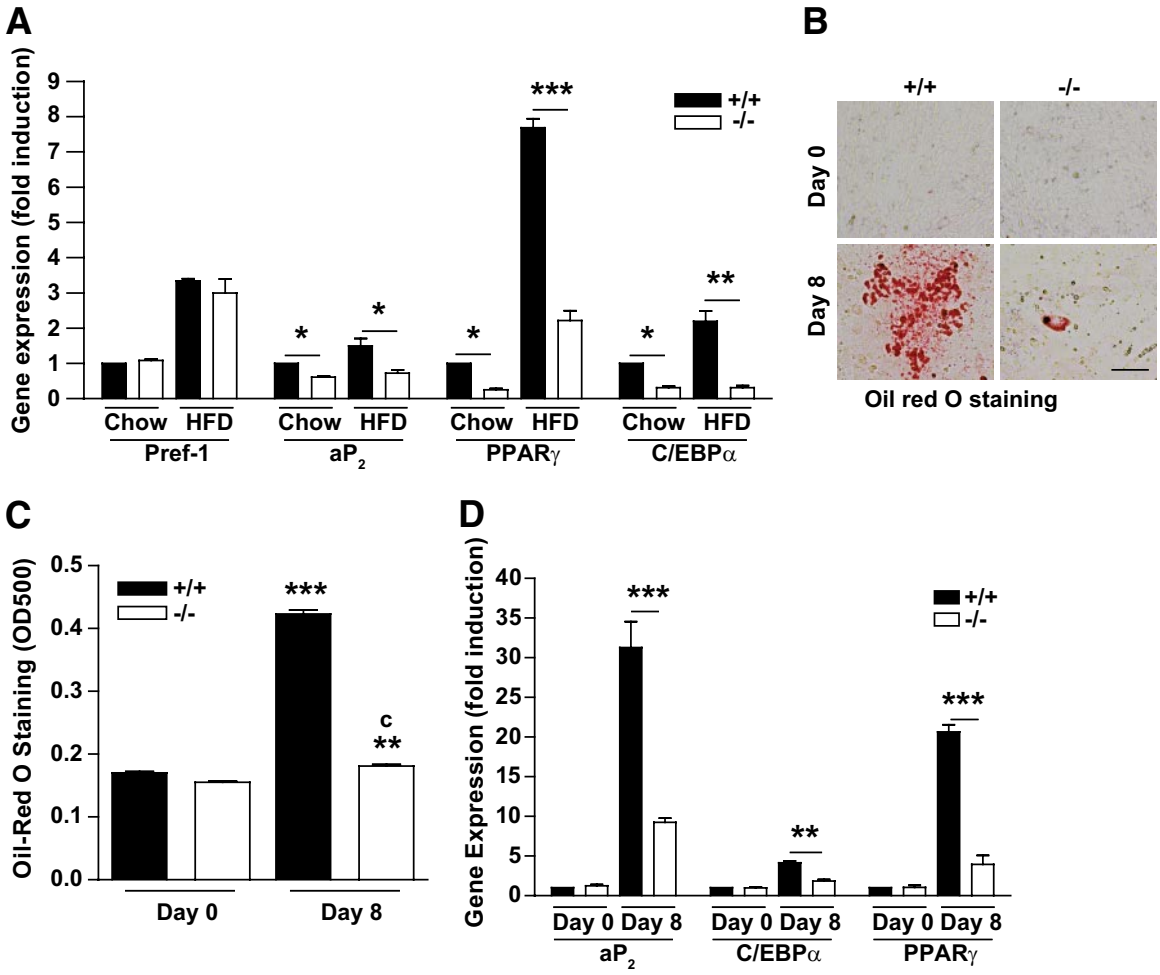

FIG. 3. PIKE is essential for adipocyte differentiation *A*: Impaired adipose gene expression in PIKE-null WAT. RNA from inguinal WAT of wild-type (+/+) and knockout (−/−) mice (8–9 months old) that have been fed chow or HFD for 20 weeks was collected and used in RT-PCR. Expression of preadipocyte markers Pref-1, mature adipocyte marker aP2, transcription factors PPARγ and C/EBPα was normalized to GAPDH. Results were expressed as fold induction against the corresponding expression level in wild-type animals fed with chow diet ($n = 3$, *$P < 0.05$; **$P < 0.01$; ***$P < 0.001$, Student t test). *B*: Oil red O staining of MEFs isolated from wild-type (+/+) and knockout (−/−) mice before (day 0) and after (day 8) induced adipocyte differentiation. Scale bar represents 50 μm. Representative result of three independent experiments is shown. *C*: Quantification of accumulated lipid in MEFs before (day 0) and after (day 8) isobutylmethylxathine-dexamethasone insulin (MDI) induction. Oil red O in the MEFs was extracted by isopropanol and measured in optical density 500 nm ($P < 0.01$, ***$P < 0.001$ vs. noninduced control of the same genotype; c: $P < 0.001$ vs. different genotype under the same treatment; one-way ANOVA, $n = 3$). *D*: Impaired adipose gene expression in PIKE-null MEFs. RNA from MEFs of wild-type (+/+) and knockout (−/−) mice before (day 0) and after (day 8) induced adipocyte differentiation. Expression of mature adipocyte marker aP2 and transcription factors PPARγ and C/EBPα was normalized to GAPDH. Results were expressed as fold induction against the corresponding expression level in day-0 wild-type MEFs ($n = 3$, **$P < 0.01$; ***$P < 0.001$, Student t test). (A high-quality digital representation of this figure is available in the online issue.)**

third, *fifth*, *sixth*, and *seventh panels*). On the other hand, insulin hypersensitivity was not detected in *PIKE*$^{-/-}$ liver (data not shown). Consistent with higher Akt phosphorylation in WAT and muscle, in vitro ^{3}H-2-deoxyglucose uptake under insulin stimulation was significantly augmented in *PIKE*$^{-/-}$ muscle and WAT (Fig. 4*F*). Together, our data suggest that *PIKE*$^{-/-}$ muscle and WAT are hypersensitive to insulin stimulation, leading to higher glucose uptake, thus protecting the mice from hyperglycemia during HFD treatment.

PIKE-A is an Akt upstream effector, which binds Akt and enhances its kinase activity in glioblastomas (6,13). It is thus anticipated that *PIKE*$^{-/-}$ mice would display diabetic phenotypes as deletion of Akt2 in mice showed impaired glucose tolerance (28). To our surprise, blood glucose level is normal in *PIKE*$^{-/-}$ mice. Because *Akt1*$^{-/-}$ or *Akt3*$^{-/-}$ mice have no obvious defect in glucose homeostasis, the normoglycemic condition in *PIKE*$^{-/-}$ mice could be explained if PIKE-A associates selectively with Akt1 and Akt3 rather than Akt2. As predicted, PIKE-A preferentially bound both Akt1 and Akt3 (supplementary Fig. 2*A*), suggesting that only Akt1 and Akt3 activities may be altered in *PIKE*$^{-/-}$ tissues. Concurrent with this notion, the brain mass of *PIKE*$^{-/-}$ mice was smaller than the control mice (supplementary Fig. 2*B*), a phenotype that is specifically observed in Akt3-null animals (29).

Lipid oxidation is enhanced in *PIKE*$^{-/-}$ mice. Animal models with lipoatrophy often associate with hyperlipidemia and ectopic lipid accumulation (30). However, significant changes in neither circulating triglyceride (Fig. 5*A*) nor ectopic lipid depositions in liver (Fig. 5*B*) were seen in the *PIKE*$^{-/-}$ mice, suggesting the excessively absorbed lipid during HFD feeding in PIKE-null animals may be metabolized rather than deposited as storage. To test this possibility, we first monitored the frequency of animal movements using open-field locomotor assay (31). Whereas the activity in wild-type mice decreased when they adapted to the test cage, physical movement of

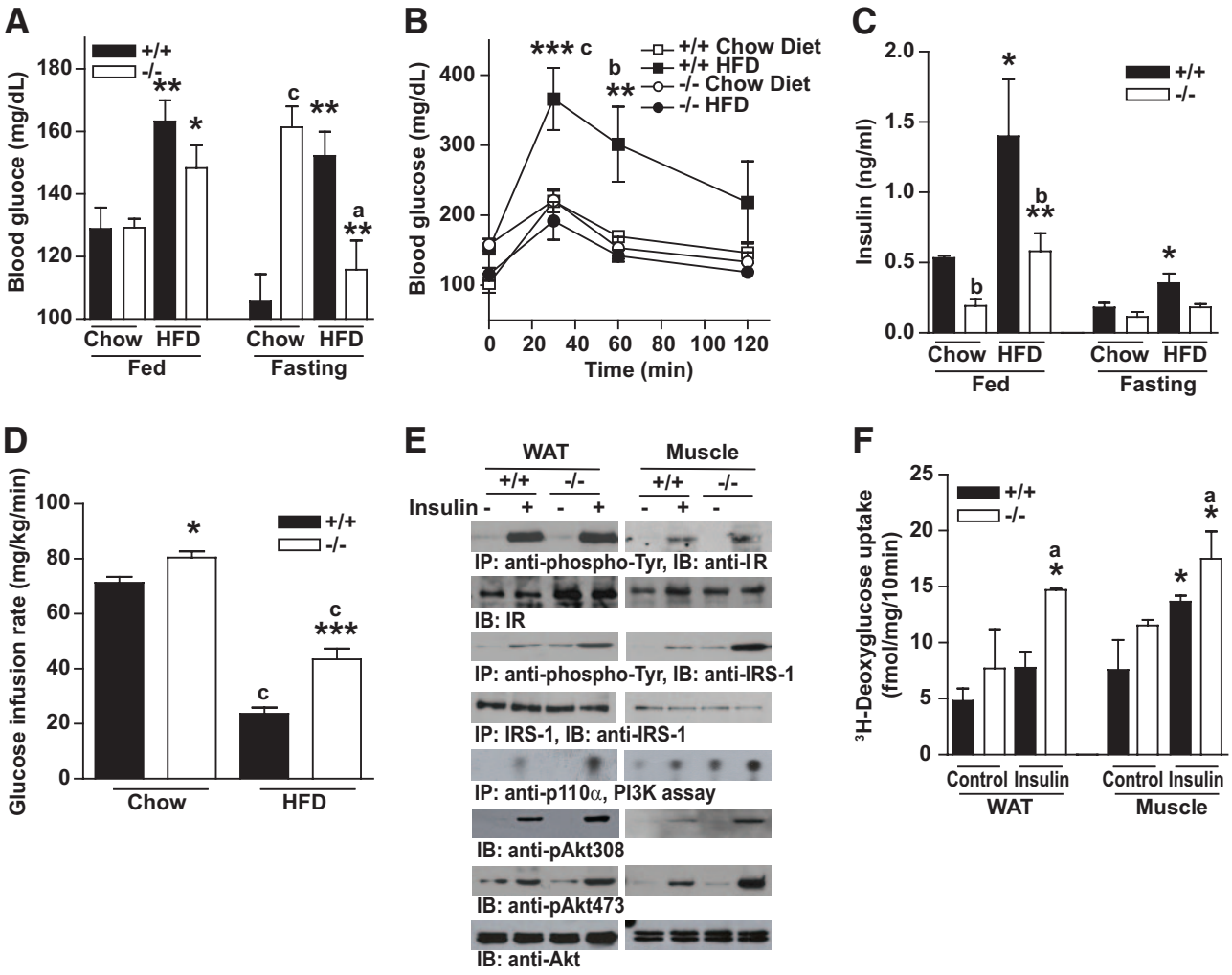

FIG. 4. *PIKE* knockout mice are protected from diet-induced hyperglycemia by enhanced systemic insulin sensitivity. *A*: Blood glucose level in fed and fasting (16 h) wild-type (+/+) and *PIKE* knockout (−/−) mice (8–9 months old) that have been fed with chow or HFD for 20 weeks. Results were expressed as mean ± SEM (*$P < 0.05$; **$P < 0.01$ vs. the same genotype treated with different diets; a: $P < 0.05$ vs. different genotypes treated with the same diet under fasting condition; c: $P < 0.001$ vs. fed and fasted $PIKE^{-/-}$ mice treated with chow diet; one-way ANOVA, $n = 4$–7). *B*: Glucose tolerance test in wild-type (+/+) and *PIKE* knockout (−/−) mice (8–9 months old) that have been fed with HFD for 20 weeks (8–9 months old) after overnight fasting. Blood glucose level was monitored at different time intervals after intraperitoneal injection of glucose (2 g/kg). Results were expressed as mean ± SEM ($n = 7$; **$P < 0.01$; ***$P < 0.05$ vs. the same genotype; b: $P < 0.01$, c: $P < 0.001$ vs. the same diet; two-way ANOVA). *C*: Circulating insulin concentration of wild-type (+/+) and knockout (−/−) mice (8–9 months old) that have been fed with chow diet or HFD for 20 weeks ($n = 4$). Results were expressed as mean ± SEM (*$P < 0.05$, **$P < 0.01$ vs. the same genotype; b: $P < 0.01$ vs. the same diet; one-way ANOVA). *D*: Glucose infusion rate in wild-type (+/+) and knockout (−/−) mice (8–9 months old) that have been fed with chow diet or HFD for 20 weeks during hyperinsulinemic-euglycemic clamp experiment. Results were expressed as mean ± SEM ($n = 9$; *$P < 0.05$, ***$P < 0.01$ vs. the same diet; c: $P < 0.001$ vs. the same genotype; one-way ANOVA). *E*: Enhanced insulin signaling in fasted 3-month-old wild-type (+/+) and PIKE-null (−/−) mice fed with chow diet. Mice were administered saline (−) or 5 units human insulin (+) via the inferior vena cava. After 5 min, inguinal WAT and skeletal muscle were isolated and frozen in liquid nitrogen. The phosphorylation of insulin receptor (*first panel*), IRS-1 (*third panel*), and Akt (Thr^{308} and Ser^{473}) (*sixth* and *seventh panels*) was determined using specific antibodies as indicated. PI 3-kinases in the tissues were precipitated using anti-p110α antibody and their activities were assayed (*fifth panel*). The expression of total insulin receptor (*second panel*), IRS-1 (*fourth panel*), and Akt (*eighth panel*) was determined to show equal loading. Representative results from three mice of each genotype were shown. *F*: Insulin elicits higher glucose uptake in fat and muscle of PIKE-null mice. Soleus muscle and inguinal WAT excised from 3- to 5-month-old wild-type (+/+) or *PIKE* knockout (−/−) mice were used in determining the ^{3}H-2-deoxyglucose uptake in the presence of 10 mU/ml human insulin. Results were presented as mean ± SEM ($n = 3$; *$P < 0.05$ vs. the same genotype; a: $P < 0.05$ vs. the same treatment, one-way ANOVA).

$PIKE^{-/-}$ mice remained substantially higher throughout the experiment in both diet conditions (Fig. 5*C*). We also examined the metabolic rate using metabolic cages (23). Respiratory exchange ratio was lower in $PIKE^{-/-}$ animals in both diet treatments, suggesting that mutant mice have a higher fatty acid catabolism (Fig. 5*D*). This suggested high lipid oxidation was further supported by the high phosphorylation level of AMPK and ACC in $PIKE^{-/-}$ muscle, brown adipose tissue (BAT), and WAT. AMPK phosphorylation was reduced after HFD feeding in wild-type BAT and WAT. However, AMPK in $PIKE^{-/-}$ WAT remained highly phosphorylated in both feeding groups (Fig. 5*E*, *first* and *tenth panels*). In parallel, phosphorylation of ACC in $PIKE^{-/-}$ BAT and WAT was higher than the control group (Fig. 5*E*, *third*, *fourth*, and *12th panels*). Whereas AMPK expression in WAT remained unchanged after HFD feeding, AMPK in BAT was greatly reduced in both genotypes (Fig. 5*E*, *second* and *11th panels*). Expression of ACC was reduced after HFD treatment in both wild-type and $PIKE^{-/-}$ BAT and WAT (Fig. 5*E*, *fifth* and *13th panels*). Interestingly, $PIKE^{-/-}$ BAT has higher ACC expression (Fig. 5*E*, *13th panel*). Similar phosphorylation pattern occurred in both AMPK and ACC in $PIKE^{-/-}$ muscle (Fig. 5*E*, *sixth* and *eighth panels*) with unchanged

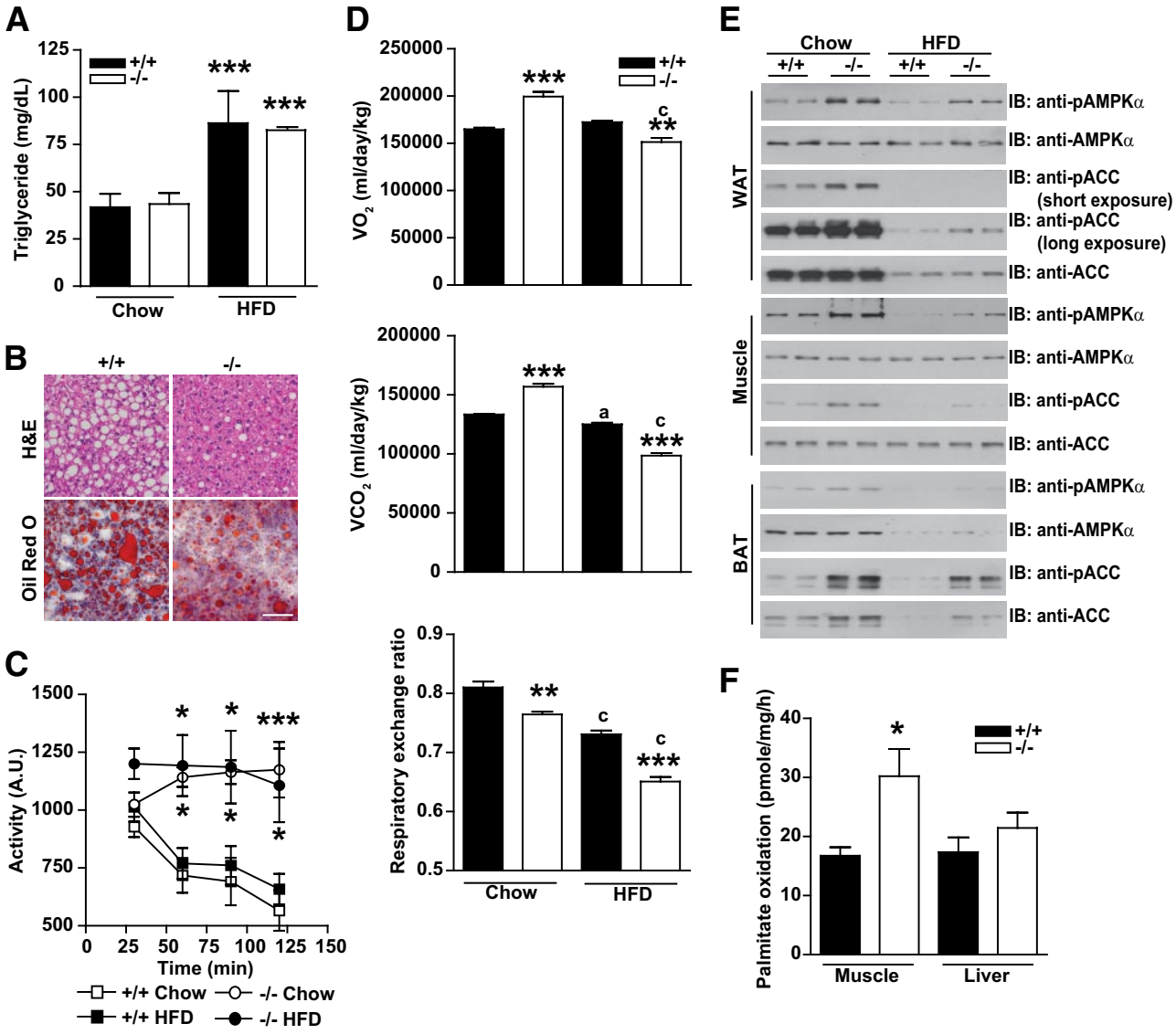

FIG. 5. Enhanced lipid oxidation in *PIKE*$^{-/-}$ mice. *A*: Serum triglyceride level of wild-type (+/+) and knockout (−/−) mice (8–9 months old) that have been fed with chow or HFD for 20 weeks. Results were expressed as mean ± SEM (n = 4; ***P < 0.001 vs. the same genotype; one-way ANOVA). *B*: Hematoxylin-eosin (H&E) (*upper panel*) and oil red O (*lower panel*) staining of liver sections collected from wild-type (+/+) and knockout (−/−) mice (8–9 months old) that have been fed with HFD for 20 weeks. Scale bar represents 50 μm. Representative result of three mice from each genotype is shown. *C*: Spontaneous activity of wild-type (+/+) and PIKE knockout (−/−) mice fed with chow or HFD for 14 weeks. Results were expressed as mean ± SEM (n = 7; *P < 0.05, ***P < 0.001 vs. the same diet). *D*: Oxygen consumption (*top panel*), CO_2 release (*middle panel*), and respiratory exchange ratio (*bottom panel*) in wild-type (solid bar) and knockout (open bar) mice fed with chow and HFD for 20 weeks (n = 4). Results were expressed as mean ± SEM (P < 0.01, ***P < 0.001 vs. the same diet; a: P < 0.05, c: P < 0.001 vs. the same genotype, one-way ANOVA, n = 4). *E*: Analysis of ACC and AMPK phosphorylation in wild-type (+/+) and knockout (−/−) mice (8–9 months old) that have been fed with chow or HFD for 20 weeks. Extracts of inguinal WAT, BAT, and muscle were prepared and immunoblotted with phosphor–Thr^{172}-AMPK, phosphor–Ser^{79}-ACC, total AMPK, and ACC antibodies. *F*: Elevated fatty acid oxidation in *PIKE*$^{-/-}$ muscle cells. Rate of ^{3}H-palmitate oxidation was measured in cultured skeletal muscle cells and hepatocytes isolated from wild-type (+/+) and PIKE knockout (−/−) mice. Results were expressed as mean ± SEM (*P < 0.05, one-way ANOVA, n = 5). (A high-quality digital representation of this figure is available in the online issue.)**

protein levels (32) (Fig. 5*E*, *seventh* and *ninth panels*). In contrast, no significant changes in hypothalamic AMPK and ACC phosphorylation were found in *PIKE*$^{-/-}$ animals in both feeding conditions (supplementary Fig. 3*A*). Moreover, AMPK and ACC phosphorylation was not enhanced in *PIKE*$^{-/-}$ MEFs (supplementary Fig. 3*B*). These results suggest a tissue-specific effect of PIKE-A in modulating AMPK and ACC activity. We have also performed the fatty acid oxidation assay in cultured *PIKE*$^{-/-}$ muscle cells and hepatocytes. In agreement with the immunoblotting analysis in Fig. 5*E*, an elevated palmitate oxidation rate was detected in *PIKE*$^{-/-}$ muscle cells but not hepatocytes (Fig. 5*F*).

Therefore, the high physical activity of *PIKE*$^{-/-}$ mice and enhanced lipid oxidation in BAT, WAT, and muscle may account for their lean phenotype during HFD feeding. The higher AMPK phosphorylation in *PIKE*$^{-/-}$ WAT also provides a possible explanation for the defective adipogenesis observed, because prolonged AICAR-induced AMPK activation inhibits adipocyte differentiation by diminishing PPARγ and C/EBPα expressions (33,34). Furthermore, agonist-activated AMPK potentiates the insulin-stimulated glucose uptake by activating IRS-1 (35,36), which may explain the enhanced PI 3-kinase and Akt activities in the muscle and WAT of *PIKE*$^{-/-}$ mice.

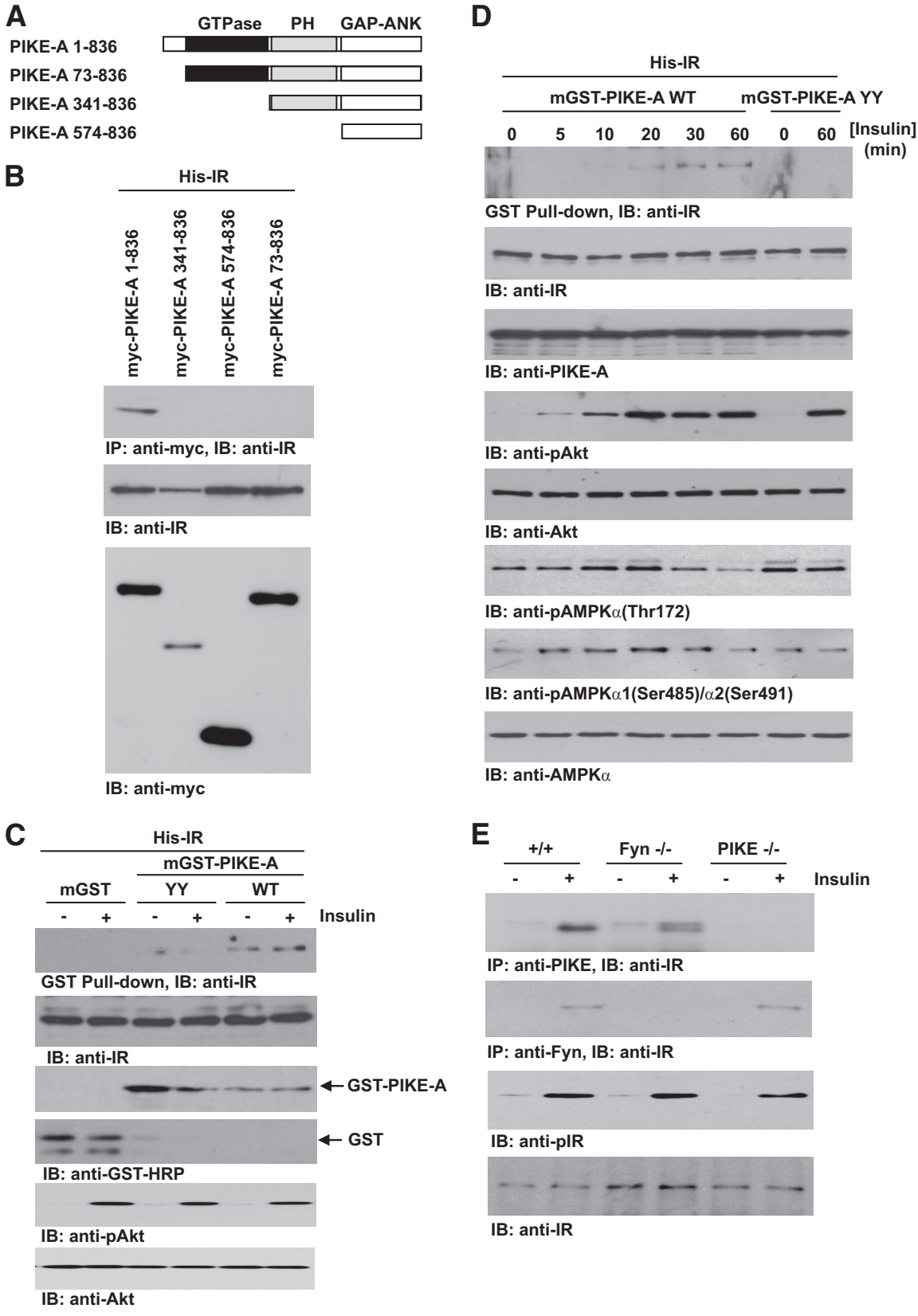

FIG. 6. PIKE interacts with insulin receptor and is essential for insulin-suppressed AMPK phosphorylation. *A*: Diagrammatic representation of various *myc*-tagged PIKE-A truncates. PIKE-A is a GTPase containing a short NH_2-terminal, a GTPase domain (GTPase) for hydrolysis of GTP, a PH domain for phosphoinositol lipid interaction, and a COOH-terminal region (GAP-ANK) with sequence homology to ARF/GAP protein and ankyrin repeats. *B*: Mapping of the insulin receptor interaction domain in PIKE-A. Various *myc*-tagged PIKE-A truncation mutants as shown in *A* and His-tagged insulin receptor (His-IR) were cotransfected into HEK293 cells. The *myc*-tagged proteins were immunoprecipitated and the associated insulin receptor was detected using anti–insulin receptor antibody (*top panel*). Expression of His-IR (*middle panel*) and various *myc*-tagged proteins (*lower panel*) was also detected. *C*: Fyn phosphorylation of PIKE-A is important for insulin receptor interaction. HEK293

PIKE-A is essential for insulin-suppressed AMPK phosphorylation. Next, we sought to clarify the role of PIKE-A in modulating AMPK phosphorylation. Fyn knockout ($Fyn^{-/-}$) mice are lipodystrophic with enhanced AMPK activity in muscle and WAT (37). These metabolic characteristics highly resemble the phenotypes of $PIKE^{-/-}$ mice. Given that PIKE-A is a substrate of Fyn (38) and Fyn interacts with IRS-1 in an insulin-dependent manner (39), we hypothesized that PIKE-A may form a complex with Fyn and insulin receptor upon insulin stimulation, which is essential for insulin to suppress AMPK activity (40,41). In HEK293 cells, PIKE-A associated with insulin receptor through its NH_2-terminal (1–72 amino acids) (Fig. 6*A* and *B*), in which their interaction could be enhanced by insulin stimulation (Fig. 6*C*, *first panel*). However, this interaction was abolished when the Fyn phosphorylation site (Tyr682 and Tyr774) in PIKE-A (PIKE-A YY) was mutated (Fig. 6*C*, *first panel*), suggesting Fyn phosphorylation is critical to the formation of PIKE-A/insulin receptor complex. The kinetics of insulin receptor/PIKE-A complex formation inversely correlated with the phosphorylation of AMPK (Fig. 6*D*, *first* and *sixth panels*). Remarkably, neither Thr^{172} nor Ser^{485}/Ser^{491} phosphorylation (42) was altered by insulin in GST-PIKE-A YY–transfected cells (Fig. 4*D*, *sixth* and *seventh panels*), suggesting that PIKE-A binding to insulin receptor is critical to mediate the inhibitory action of insulin on AMPK phosphorylation. On the other hand, Akt phosphorylation was not affected in either wild-type PIKE-A or PIKE-A YY cells in response to insulin (Fig. 6*D*, *fourth panel*). The formation of PIKE/insulin receptor/Fyn complex was further demonstrated in muscle tissue. In vivo insulin injection in wild-type mice enhanced the formation of PIKE-A/insulin receptor complex, which was substantially reduced in $Fyn^{-/-}$ tissue (Fig. 4*G*, *first panel*). This complex was not detected in PIKE-null tissues (Fig. 6*E*, *first panel*). Our immunoprecipitation results also confirmed that the association of Fyn and insulin receptor in muscle is insulin dependent (Fig. 6*E*, *second panel*). Furthermore, the formation of Fyn/insulin receptor complex was not affected in *PIKE*-null tissues, suggesting that PIKE-A is not essential for their interaction (Fig. 6*E*, *second panel*). Thus, the interaction between PIKE-A and insulin receptor is important for insulin to suppress AMPK phosphorylation, which provides a possible explanation to the enhanced AMPK phosphorylation in $PIKE^{-/-}$ WAT and muscle.

DISCUSSION

One of the major findings in the current report is that PIKE-A is critical for adipocyte differentiation. Several lines of evidence support the role of PIKE-A in terminal adipocyte differentiation instead of preadipocyte formation. First, the mature adipocyte marker aP2 is significantly decreased during in vitro adipocyte differentiation in $PIKE^{-/-}$ MEFs, indicating PIKE-A is important for adipocyte differentiation (Fig. 3*B* and *C*). Second, PIKE-A expression is increased in fat tissue development of HFD-fed and *ob/ob* mice, which highlights its function in the process (Fig. 2*H*). Lastly, HFD induced comparable preadipocyte marker Pref-1 expression in both wild-type and $PIKE^{-/-}$ mice, indicating that formation of new adipocytes is normal in PIKE-null adipose tissue (Fig. 3*A*). Interestingly, we found a small portion of $PIKE^{-/-}$ MEFs was able to differentiate into mature adipocytes (Fig. 3*B*), and quantitative analysis revealed a small but statistically significant increment of lipid accumulation in $PIKE^{-/-}$ MEFs (Fig. 3*C*). This result indicates that a PIKE-A–independent mechanism is responsible for some adipocyte differentiation, which also accounts for the existence but not completely the absence of adipose tissue in $PIKE^{-/-}$ mice.

Ectopic lipid storage due to adipocyte differentiation defect is associated with hyperlipidemia and liver steatosis (43). However, we could not detect these pathologic conditions in $PIKE^{-/-}$ mice (Fig. 5*A* and *B*). It is thus reasonable to predict that the lipid spillover from adipocyte is metabolized in mutant animals. Our results that PIKE-null fat and muscle have significantly elevated AMPK and ACC phosphorylation suggest an elevated β-oxidation in these tissues (Fig. 5*E*), which is further supported by the enhanced fatty acid oxidation rate in the in vitro assay (Fig. 5*F*) and the low respiratory exchange ratio values (Fig. 5*D*). AMPK has been viewed as a fuel sensor for glucose and lipid metabolism. Once activated, AMPK initiates a concomitant inhibition of energy-consuming biosynthetic pathways and activation of ATP-producing pathways such as fatty oxidation in mitochondria (44). As a result, most of the lipids absorbed in $PIKE^{-/-}$ mice are oxidized as the energy source, which accounts for the lean phenotype during the HFD treatment.

The uplifted phosphorylation of AMPK and its downstream substrate ACC in PIKE-null muscle and adipose tissues indicates that PIKE-A negatively regulates the activities of these enzymes. This notion is further supported by the fact that PIKE-A is critical for insulin to inhibit AMPK phosphorylation in 293 cells (Fig. 6*D*). This upregulation of AMPK activity in $PIKE^{-/-}$ muscle and fat also provides a possible mechanism accounting for the elevated systemic insulin sensitivity, as AMPK and insulin signaling are intimately connected. Agonist-induced AMPK activation increases the glucose uptake in muscle (45). It also potentiates the insulin-stimulated glucose uptake by activating IRS-1 (35,36). A similar observation was made in

cells were cotransfected with His-IR and GST alone, GST-tagged wild-type PIKE-A (WT), or Tyr682, 774F (YY) mutant. The GST proteins were pulled down by glutathione beads and the associated insulin receptor was examined using anti–insulin receptor antibody (*first panel*). Expression of His-IR (*second panel*) and various GST-tagged proteins (*third* and *fourth panels*) was detected. Phosphorylation of Akt (Ser^{473}) was also examined to verify insulin action (*fifth panel*). Total Akt expression was checked as an indication of equal loading (*sixth panel*). *D*: Mutation of Fyn phosphorylation site impairs insulin-suppressed AMPK phosphorylation. HEK293 cells were first transfected with GST-tagged wild-type PIKE-A (WT) or Tyr682, 774F mutant (YY). After serum starvation for 24 h, the cells were stimulated with 100 nmol/l insulin for different time intervals. The PIKE proteins were pulled down by glutathione beads, and the associated insulin receptor was detected using anti–insulin receptor antibody (*first panel*). The phosphorylation of Akt (Ser^{473}; *fourth panel*), AMPKα (Thr^{172}; *sixth panel*), and AMPKα1 (Ser^{485})/AMPKα2 (Ser^{491}; *seventh panel*) was determined using specific antibodies. Expression of His-IR (*second panel*) and GST-PIKE-A (*third panel*) was verified. The amount of Akt (*fifth panel*) and AMPK (*eighth panel*) was detected to show equal loading. *E*: Insulin enhances PIKE-A and insulin receptor interaction in muscle. Overnight-fasted wild-type (+/+), Fyn knockout ($Fyn^{-/-}$), and PIKE knockout ($PIKE^{-/-}$) mice (3–4 months old) were injected with saline (−) or 5 units human insulin (+) through the inferior vena cava for 5 min. The muscles were then collected and homogenized, and the PIKE-A was immunoprecipitated using anti-PIKE antibody. The associated insulin receptor was detected using anti–insulin receptor antibody (*first panel*). The interaction of Fyn and insulin receptor was also examined by immunoprecipitation using anti-Fyn antibody (*second panel*). Phosphorylation of insulin receptor was examined as an indication of insulin stimulation (*third panel*). Total insulin receptor was also detected to indicate loading (*fourth panel*).

adipose tissue that treatment of adipocytes with AMPK agonist AICAR enhanced basal glucose uptake by increasing GLUT4 translocation (46). Long-term activation of AMPK in mice increases the systemic insulin sensitivity and protects animals from HFD-induced obesity and diabetes (34,47), which is in agreement with our observations in *PIKE*$^{-/-}$ mice. It is noteworthy that the alleviated insulin resistance in *PIKE*$^{-/-}$ mice after HFD treatment may be a result of reduced inflammation. Because reduced circulating TNF-α could improve insulin sensitivity and increase AMPK activity (48,49), the low blood TNF-α in *PIKE*$^{-/-}$ mice (Fig. 2*G*) may also contribute significantly to improve the diet-induced insulin resistance.

Because the whole-body–knockout mice were used in the present study, we cannot exclude the possibility that deletion of PIKE-A in the brain causes a central effect to modify whole-body activity and metabolism. Because brain is the major site to control appetite and body weight (50), where PIKE is highly expressed (Fig. 1*D*), it is reasonable to suspect that reduced food intake (Fig. 2*B*) and elevated physical activity (Fig. 5*C*) in *PIKE*$^{-/-}$ mice are the primary causes of lean phenotype during HFD treatment. However, our data strongly support that peripheral ablation of PIKE-A does play a role in preventing obesity development. First, the feeding behavior is comparable between wild-type and *PIKE*$^{-/-}$ mice fed a chow diet, when lipoatrophy is already obvious. Second, induced differentiation in *PIKE*$^{-/-}$ MEFs is greatly impaired (Fig. 3*B*), suggesting ablation of PIKE per se in MEFs is adequate to suppress adipogenesis. Third, PIKE-A interacts with the insulin receptor in a Fyn-dependent manner, which is essential for insulin-induced AMPK phosphorylation in muscle (Fig. 6*D*). Deletion of PIKE in muscle, therefore, would enhance the AMPK phosphorylation and lipid oxidation (Fig. 5*E* and *F*). Lastly, isolated *PIKE*$^{-/-}$ WAT and muscle, in which the metabolic influence by the brain is eliminated, have higher ^{3}H-2-deoxyglucose uptake when stimulated by insulin (Fig. 4*F*).

Our data also suggest that the function of PIKE-A is not restricted to enhance Akt activity alone. We have demonstrated that PIKE-A physically interacts with the insulin receptor, which is important for insulin to suppress AMPK phosphorylation. Our data also provide a novel mechanistic insight into the phenotypes observed in *Fyn*$^{-/-}$ mice (37), as PIKE-A/insulin receptor association is Fyn dependent. Conceivably, PIKE-A is a downstream target of Fyn that inhibits the activity of AMPK during obesity development. Thus, PIKE-A may represent an additional regulatory point, in addition to Akt, for insulin to suppress AMPK phosphorylation.

In all, our results uncover the novel physiological functions of PIKE-A, which plays important roles in obesity development and the accompanied insulin resistance by regulating AMPK activities negatively. Consequently, less fat is deposited and the associated insulin resistance is ameliorated. Therefore, PIKE-A may represent a potential therapeutic target for obesity and the adjunct insulin resistance.

ACKNOWLEDGMENTS

K.Y. has received a grant from the National Institutes of Health RO1 (NS-045627).

No potential conflicts of interest relevant to this article were reported.

Parts of this study were presented in poster form at the 69th Scientific Sessions of the American Diabetes Association, New Orleans, Louisiana, 5–9 June 2009.

REFERENCES

1. Brown WV, Fujioka K, Wilson PW, Woodworth KA. Obesity: why be concerned? Am J Med 2009;122:S4–S11
2. Kelly T, Yang W, Chen CS, Reynolds K, He J. Global burden of obesity in 2005 and projections to 2030. Int J Obes (Lond) 2008;32:1431–1437
3. Ichihara S, Yamada Y. Genetic factors for human obesity. Cell Mol Life Sci 2008;65:1086–1098
4. Bossé Y, Chagnon YC, Després JP, Rice T, Rao DC, Bouchard C, Pérusse L, Vohl MC. Genome-wide linkage scan reveals multiple susceptibility loci influencing lipid and lipoprotein levels in the Quebec Family Study. J Lipid Res 2004;45:419–426
5. Collaku A, Rankinen T, Rice T, Leon AS, Rao DC, Skinner JS, Wilmore JH, Bouchard C. A genome-wide linkage scan for dietary energy and nutrient intakes: the Health, Risk Factors, Exercise Training, and Genetics (HERITAGE) Family Study. Am J Clin Nutr 2004;79:881–886
6. Ahn JY, Rong R, Kroll TG, Van Meir EG, Snyder SH, Ye K. PIKE (phosphatidylinositol 3-kinase enhancer)-A GTPase stimulates Akt activity and mediates cellular invasion. J Biol Chem 2004;279:16441–16451
7. Ye K, Aghdasi B, Luo HR, Moriarity JL, Wu FY, Hong JJ, Hurt KJ, Bae SS, Suh PG, Snyder SH. Phospholipase C gamma 1 is a physiological guanine nucleotide exchange factor for the nuclear GTPase PIKE. Nature 2002;415:541–544
8. Ye K, Aghdasi B, Luo HR, Moriarity JL, Wu FY, Hong JJ, Hurt KJ, Bae SS, Suh PG, Snyder SH. Pike: a nuclear gtpase that enhances PI3kinase activity and is regulated by protein 4.1N. Cell 2000;103:919–930
9. Xia C, Ma W, Stafford LJ, Liu C, Gong L, Martin JF, Liu M. GGAPs, a new family of bifunctional GTP-binding and GTPase-activating proteins. Mol Cell Biol 2003;23:2476–2488
10. Nagase T, Seki N, Ishikawa K, Tanaka A, Nomura N. Prediction of the coding sequences of unidentified human genes: V, the coding sequences of 40 new genes (KIAA0161-KIAA0200) deduced by analysis of cDNA clones from human cell line KG-1. DNA Res 1996;3:17–24
11. Rong R, Ahn JY, Huang H, Nagata E, Kalman D, Kapp JA, Tu J, Worley PF, Snyder SH, Ye K. PI3 kinase enhancer-Homer complex couples mGluRI to PI3 kinase, preventing neuronal apoptosis. Nat Neurosci 2003;6:1153–1161
12. Tang X, Jang SW, Okada M, Chan CB, Feng Y, Liu Y, Luo SW, Hong Y, Rama N, Xiong WC, Mehlen P, Ye K. Netrin-1 mediates neuronal survival through PIKE-L interaction with the dependence receptor UNC5B. Nat Cell Biol 2008;10:698–706
13. Ahn JY, Hu Y, Kroll TG, Allard P, Ye K. PIKE-A is amplified in human cancers and prevents apoptosis by up-regulating Akt. Proc Natl Acad Sci U S A 2004;101:6993–6998
14. Liu R, Tian B, Gearing M, Hunter S, Ye K, Mao Z. Cdk5-mediated regulation of the PIKE-A-Akt pathway and glioblastoma cell invasion. Proc Natl Acad Sci U S A 2008;105:7570–7575
15. Brookheart RT, Michel CI, Schaffer JE. As a matter of fat. Cell Metab 2009;10:9–12
16. Lage R, Diéguez C, Vidal-Puig A, López M. AMPK: a metabolic gauge regulating whole-body energy homeostasis. Trends Mol Med 2008;14:539–549
17. Zhang BB, Zhou G, Li C. AMPK: an emerging drug target for diabetes and the metabolic syndrome. Cell Metab 2009;9:407–416
18. Ye K, Compton DA, Lai MM, Walensky LD, Snyder SH. Protein 4.1N binding to nuclear mitotic apparatus protein in PC12 cells mediates the antiproliferative actions of nerve growth factor. J Neurosci 1999;19:10747–10756
19. Chan CB, Cheng CH. Identification and functional characterization of two alternatively spliced growth hormone secretagogue receptor transcripts from the pituitary of black seabream Acanthopagrus schlegeli. Mol Cell Endocrinol 2004;214:81–95
20. Chang PY, Jensen J, Printz RL, Granner DK, Ivy JL, Moller DE. Overexpression of hexokinase II in transgenic mice: evidence that increased phosphorylation augments muscle glucose uptake. J Biol Chem 1996;271:14834–14839
21. An JJ, Rhee Y, Kim SH, Kim DM, Han DH, Hwang JH, Jin YJ, Cha BS, Baik JH, Lee WT, Lim SK. Peripheral effect of alpha-melanocyte-stimulating hormone on fatty acid oxidation in skeletal muscle. J Biol Chem 2007;282:2862–2870
22. Kim HJ, Higashimori T, Park SY, Choi H, Dong J, Kim YJ, Noh HL, Cho YR, Cline G, Kim YB, Kim JK. Differential effects of interleukin-6 and -10 on skeletal muscle and liver insulin action in vivo. Diabetes 2004;53:1060–1067
23. Hong EG, Jung DY, Ko HJ, Zhang Z, Ma Z, Jun JY, Kim JH, Sumner AD, Vary TC, Gardner TW, Bronson SK, Kim JK. Nonobese, insulin-deficient

Ins2Akita mice develop type 2 diabetes phenotypes including insulin resistance and cardiac remodeling. Am J Physiol Endocrinol Metab 2007;293:E1687–E1696
24. Wu Z, Rosen ED, Brun R, Hauser S, Adelmant G, Troy AE, McKeon C, Darlington GJ, Spiegelman BM. Cross-regulation of C/EBP alpha and PPAR gamma controls the transcriptional pathway of adipogenesis and insulin sensitivity. Mol Cell 1999;3:151–158
25. Wang ND, Finegold MJ, Bradley A, Ou CN, Abdelsayed SV, Wilde MD, Taylor LR, Wilson DR, Darlington GJ. Impaired energy homeostasis in C/EBP alpha knockout mice. Science 1995;269:1108–1112
26. Guilherme A, Virbasius JV, Puri V, Czech MP. Adipocyte dysfunctions linking obesity to insulin resistance and type 2 diabetes. Nat Rev Mol Cell Biol 2008;9:367–377
27. Michael MD, Kulkarni RN, Postic C, Previs SF, Shulman GI, Magnuson MA, Kahn CR. Loss of insulin signaling in hepatocytes leads to severe insulin resistance and progressive hepatic dysfunction. Mol Cell 2000;6:87–97
28. Cho H, Mu J, Kim JK, Thorvaldsen JL, Chu Q, Crenshaw EB III, Kaestner KH, Bartolomei MS, Shulman GI, Birnbaum MJ. Insulin resistance and a diabetes mellitus-like syndrome in mice lacking the protein kinase Akt2 (PKB beta). Science 2001;292:1728–1731
29. Tschopp O, Yang ZZ, Brodbeck D, Dummler BA, Hemmings-Mieszczak M, Watanabe T, Michaelis T, Frahm J, Hemmings BA. Essential role of protein kinase B gamma (PKB gamma/Akt3) in postnatal brain development but not in glucose homeostasis. Development 2005;132:2943–2954
30. He W, Barak Y, Hevener A, Olson P, Liao D, Le J, Nelson M, Ong E, Olefsky JM, Evans RM. Adipose-specific peroxisome proliferator-activated receptor gamma knockout causes insulin resistance in fat and liver but not in muscle. Proc Natl Acad Sci U S A 2003;100:15712–15717
31. Mitchell HA, Bogenpohl JW, Liles LC, Epstein MP, Bozyczko-Coyne D, Williams M, Weinshenker D. Behavioral responses of dopamine beta-hydroxylase knockout mice to modafinil suggest a dual noradrenergic-dopaminergic mechanism of action. Pharmacol Biochem Behav 2008;91:217–222
32. Barnea M, Shamay A, Stark AH, Madar Z. A high-fat diet has a tissue-specific effect on adiponectin and related enzyme expression. Obesity (Silver Spring) 2006;14:2145–2153
33. Habinowski SA, Witters LA. The effects of AICAR on adipocyte differentiation of 3T3-L1 cells. Biochem Biophys Res Commun 2001;286:852–856
34. Giri S, Rattan R, Haq E, Khan M, Yasmin R, Won JS, Key L, Singh AK, Singh I. AICAR inhibits adipocyte differentiation in 3T3L1 and restores metabolic alterations in diet-induced obesity mice model. Nutr Metab (Lond) 2006;3:31
35. Jakobsen SN, Hardie DG, Morrice N, Tornqvist HE. 5′-AMP-activated protein kinase phosphorylates IRS-1 on Ser-789 in mouse C2C12 myotubes in response to 5-aminoimidazole-4-carboxamide riboside. J Biol Chem 2001;276:46912–46916
36. Ju JS, Gitcho MA, Casmaer CA, Patil PB, Han DG, Spencer SA, Fisher JS. Potentiation of insulin-stimulated glucose transport by the AMP-activated protein kinase. Am J Physiol Cell Physiol 2007;292:C564–C572
37. Bastie CC, Zong H, Xu J, Busa B, Judex S, Kurland IJ, Pessin JE. Integrative metabolic regulation of peripheral tissue fatty acid oxidation by the SRC kinase family member Fyn. Cell Metab 2007;5:371–381
38. Tang X, Feng Y, Ye K. Src-family tyrosine kinase fyn phosphorylates phosphatidylinositol 3-kinase enhancer-activating Akt, preventing its apoptotic cleavage and promoting cell survival. Cell Death Differ 2007;14:368–377
39. Sun XJ, Pons S, Asano T, Myers MG Jr, Glasheen E, White MF. The Fyn tyrosine kinase binds Irs-1 and forms a distinct signaling complex during insulin stimulation. J Biol Chem 1996;271:10583–10587
40. Gamble J, Lopaschuk GD. Insulin inhibition of 5′ adenosine monophosphate-activated protein kinase in the heart results in activation of acetyl coenzyme A carboxylase and inhibition of fatty acid oxidation. Metabolism 1997;46:1270–1274
41. Witters LA, Kemp BE. Insulin activation of acetyl-CoA carboxylase accompanied by inhibition of the 5′-AMP-activated protein kinase. J Biol Chem 1992;267:2864–2867
42. Horman S, Vertommen D, Heath R, Neumann D, Mouton V, Woods A, Schlattner U, Wallimann T, Carling D, Hue L, Rider MH. Insulin antagonizes ischemia-induced Thr^{172} phosphorylation of AMP-activated protein kinase alpha-subunits in heart via hierarchical phosphorylation of Ser485/491. J Biol Chem 2006;281:5335–5340
43. Savage DB, Petersen KF, Shulman GI. Disordered lipid metabolism and the pathogenesis of insulin resistance. Physiol Rev 2007;87:507–520
44. Viollet B, Foretz M, Guigas B, Horman S, Dentin R, Bertrand L, Hue L, Andreelli F. Activation of AMP-activated protein kinase in the liver: a new strategy for the management of metabolic hepatic disorders. J Physiol 2006;574:41–53
45. Merrill GF, Kurth EJ, Hardie DG, Winder WW. AICA riboside increases AMP-activated protein kinase, fatty acid oxidation, and glucose uptake in rat muscle. Am J Physiol 1997;273:E1107–E1112
46. Yamaguchi S, Katahira H, Ozawa S, Nakamichi Y, Tanaka T, Shimoyama T, Takahashi K, Yoshimoto K, Imaizumi MO, Nagamatsu S, Ishida H. Activators of AMP-activated protein kinase enhance GLUT4 translocation and its glucose transport activity in 3T3-L1 adipocytes. Am J Physiol Endocrinol Metab 2005;289:E643–E649
47. Pold R, Jensen LS, Jessen N, Buhl ES, Schmitz O, Flyvbjerg A, Fujii N, Goodyear LJ, Gotfredsen CF, Brand CL, Lund S. Long-term AICAR administration and exercise prevents diabetes in ZDF rats. Diabetes 2005;54:928–934
48. Steinberg GR, Michell BJ, van Denderen BJ, Watt MJ, Carey AL, Fam BC, Andrikopoulos S, Proietto J, Gorgun CZ, Carling D, Hotamisligil GS, Febbraio MA, Kay TW, Kemp BE. Tumor necrosis factor alpha-induced skeletal muscle insulin resistance involves suppression of AMP-kinase signaling. Cell Metab 2006;4:465–474
49. Uysal KT, Wiesbrock SM, Marino MW, Hotamisligil GS. Protection from obesity-induced insulin resistance in mice lacking TNF-alpha function. Nature 1997;389:610–614
50. Morton GJ, Cummings DE, Baskin DG, Barsh GS, Schwartz MW. Central nervous system control of food intake and body weight. Nature 2006;443:289–295